Supplemental Material

General expressions for $R_{1\rho}$ relaxation for *N*-site chemical exchange and the special case of linear chains

Hans Koss[1], Mark Rance[2] and Arthur G. Palmer, III[1]

[1]Department of Biochemistry and Molecular Biophysics, Columbia University, 630 West 168th Street, New York, NY 10032

[2]Department of Molecular Genetics, Biochemistry and Microbiology, University of Cincinnati, Cincinnati, OH 45267

I. Reduction of the 12×12 linear four-site mechanism evolution matrix to a 3×3 matrix

The evolution matrix for the linear four-site exchange mechanism is:

$$\mathbf{L}+\mathbf{K}=\begin{pmatrix}\mathbf{L}_A & 0 & 0 & 0\\ 0 & \mathbf{L}_B & 0 & 0\\ 0 & 0 & \mathbf{L}_C & 0\\ 0 & 0 & 0 & \mathbf{L}_D\end{pmatrix}+\begin{pmatrix}-k_{12} & k_{21} & 0 & 0\\ k_{12} & -k_{21}-k_{13} & k_{31} & 0\\ 0 & k_{13} & -k_{31}-k_{34} & k_{43}\\ 0 & 0 & k_{34} & -k_{43}\end{pmatrix}\otimes\mathbf{I} \tag{S1}$$

The first application of the matrix determinant lemma yields:

$$\begin{aligned}
0&=\left|\mathbf{L}+\mathbf{K}-\lambda\mathbf{I}\right|\\
&=\left|\mathbf{L}_A-\lambda\mathbf{I}\right|\left|\mathbf{L}_B-\lambda\mathbf{I}\right|\left|\mathbf{L}_C-\lambda\mathbf{I}\right|\left|\mathbf{L}_D-\lambda\mathbf{I}\right|\\
&\times\left|\mathbf{I}+\begin{pmatrix}-k_{12} & k_{21} & 0 & 0\\ 0 & -k_{13} & k_{31} & 0\\ 0 & 0 & -k_{34} & k_{43}\end{pmatrix}\begin{pmatrix}\left(\mathbf{L}_A-\lambda\mathbf{I}\right)^{-1} & 0 & 0 & 0\\ 0 & \left(\mathbf{L}_B-\lambda\mathbf{I}\right)^{-1} & 0 & 0\\ 0 & 0 & \left(\mathbf{L}_C-\lambda\mathbf{I}\right)^{-1} & 0\\ 0 & 0 & 0 & \left(\mathbf{L}_D-\lambda\mathbf{I}\right)^{-1}\end{pmatrix}\begin{pmatrix}1 & 0 & 0\\ -1 & 1 & 0\\ 0 & -1 & 1\\ 0 & 0 & -1\end{pmatrix}\right|\\
&=\left|\mathbf{L}_A-\lambda\mathbf{I}\right|\left|\mathbf{L}_B-\lambda\mathbf{I}\right|\left|\mathbf{L}_C-\lambda\mathbf{I}\right|\left|\mathbf{L}_D-\lambda\mathbf{I}\right|\\
&\times\left|\begin{pmatrix}\mathbf{I}-k_{12}\left(\mathbf{L}_A-\lambda\mathbf{I}\right)^{-1}-k_{21}\left(\mathbf{L}_A-\lambda\mathbf{I}\right)^{-1} & k_{21}\left(\mathbf{L}_B-\lambda\mathbf{I}\right)^{-1} & 0\\ k_{13}\left(\mathbf{L}_B-\lambda\mathbf{I}\right)^{-1} & \mathbf{I}-k_{13}\left(\mathbf{L}_B-\lambda\mathbf{I}\right)^{-1}-k_{31}\left(\mathbf{L}_C-\lambda\mathbf{I}\right)^{-1} & k_{31}\left(\mathbf{L}_C-\lambda\mathbf{I}\right)^{-1}\\ 0 & k_{34}\left(\mathbf{L}_C-\lambda\mathbf{I}\right)^{-1} & -k_{34}\left(\mathbf{L}_C-\lambda\mathbf{I}\right)^{-1}-k_{43}\left(\mathbf{L}_D-\lambda\mathbf{I}\right)^{-1}\end{pmatrix}\right|\\
&=\left|\mathbf{L}_A-\lambda\mathbf{I}\right|\left|\mathbf{L}_B-\lambda\mathbf{I}\right|\left|\mathbf{L}_C-\lambda\mathbf{I}\right|\left|\mathbf{L}_D-\lambda\mathbf{I}\right|\\
&\times\left|\begin{pmatrix}\mathbf{I}-k_{12}\left(\mathbf{L}_A-\lambda\mathbf{I}\right)^{-1} & 0 & 0\\ 0 & \mathbf{I} & 0\\ 0 & 0 & \mathbf{I}-k_{43}\left(\mathbf{L}_D-\lambda\mathbf{I}\right)^{-1}\end{pmatrix}\right.\\
&\left.+\begin{pmatrix}\mathbf{I}-k_{21}\left(\mathbf{L}_B-\lambda\mathbf{I}\right)^{-1} & k_{21}\left(\mathbf{L}_B-\lambda\mathbf{I}\right)^{-1} & 0\\ k_{13}\left(\mathbf{L}_B-\lambda\mathbf{I}\right)^{-1} & \mathbf{I}-k_{13}\left(\mathbf{L}_B-\lambda\mathbf{I}\right)^{-1}-k_{31}\left(\mathbf{L}_C-\lambda\mathbf{I}\right)^{-1} & k_{31}\left(\mathbf{L}_C-\lambda\mathbf{I}\right)^{-1}\\ 0 & k_{34}\left(\mathbf{L}_C-\lambda\mathbf{I}\right)^{-1} & -k_{34}\left(\mathbf{L}_C-\lambda\mathbf{I}\right)^{-1}\end{pmatrix}\right|
\end{aligned} \tag{S2}$$

The second application of the matrix determinant lemma yields:

$$
\begin{aligned}
0 &= \left|\mathbf{L}_A-\lambda\mathbf{I}\right|\left|\mathbf{L}_B-\lambda\mathbf{I}\right|\left|\mathbf{L}_C-\lambda\mathbf{I}\right|\left|\mathbf{L}_D-\lambda\mathbf{I}\right|\left|\mathbf{I}-k_{12}\left(\mathbf{L}_A-\lambda\mathbf{I}\right)^{-1}\right|\left|\mathbf{I}-k_{43}\left(\mathbf{L}_D-\lambda\mathbf{I}\right)^{-1}\right| \\
&\times\left|\mathbf{I}+\begin{pmatrix} -\left(\mathbf{L}_B-\lambda\mathbf{I}\right)^{-1} & \left(\mathbf{L}_B-\lambda\mathbf{I}\right)^{-1} & 0 \\ 0 & \left(\mathbf{L}_C-\lambda\mathbf{I}\right)^{-1} & -\left(\mathbf{L}_C-\lambda\mathbf{I}\right)^{-1} \end{pmatrix}\right. \\
&\left.\times\begin{pmatrix} \mathbf{I}-k_{12}\left(\mathbf{L}_A-\lambda\mathbf{I}\right)^{-1} & 0 & 0 \\ 0 & \mathbf{I} & 0 \\ 0 & 0 & \mathbf{I}-k_{43}\left(\mathbf{L}_D-\lambda\mathbf{I}\right)^{-1} \end{pmatrix}\begin{pmatrix} k_{21} & 0 \\ -k_{13} & -k_{31} \\ 0 & k_{34} \end{pmatrix}\right| \\
&= \left|\mathbf{L}_A-\lambda\mathbf{I}\right|\left|\mathbf{L}_B-\lambda\mathbf{I}\right|\left|\mathbf{L}_C-\lambda\mathbf{I}\right|\left|\mathbf{L}_D-\lambda\mathbf{I}\right|\left|\mathbf{I}-k_{12}\left(\mathbf{L}_A-\lambda\mathbf{I}\right)^{-1}\right|\left|\mathbf{I}-k_{43}\left(\mathbf{L}_D-\lambda\mathbf{I}\right)^{-1}\right| \\
&\times\left|\begin{pmatrix} \mathbf{I}-k_{21}\left(\mathbf{L}_B-\lambda\mathbf{I}\right)^{-1}\left(\mathbf{I}-k_{12}\left(\mathbf{L}_A-\lambda\mathbf{I}\right)^{-1}\right)-k_{13}\left(\mathbf{L}_B-\lambda\mathbf{I}\right)^{-1} & -k_{31}\left(\mathbf{L}_B-\lambda\mathbf{I}\right)^{-1} \\ -k_{13}\left(\mathbf{L}_C-\lambda\mathbf{I}\right)^{-1} & \mathbf{I}-k_{31}\left(\mathbf{L}_C-\lambda\mathbf{I}\right)^{-1}-k_{34}\left(\mathbf{L}_C-\lambda\mathbf{I}\right)^{-1}\left(\mathbf{I}-k_{43}\left(\mathbf{L}_D-\lambda\mathbf{I}\right)^{-1}\right) \end{pmatrix}\right| \\
&= \left|\mathbf{L}_A-\lambda\mathbf{I}\right|\left|\mathbf{L}_B-\lambda\mathbf{I}\right|\left|\mathbf{L}_C-\lambda\mathbf{I}\right|\left|\mathbf{L}_D-\lambda\mathbf{I}\right|\left|\mathbf{I}-k_{12}\left(\mathbf{L}_A-\lambda\mathbf{I}\right)^{-1}\right|\left|\mathbf{I}-k_{43}\left(\mathbf{L}_D-\lambda\mathbf{I}\right)^{-1}\right| \\
&\times\left|\begin{pmatrix} \mathbf{I}-k_{21}\left(\mathbf{L}_B-\lambda\mathbf{I}\right)^{-1}\left(\mathbf{I}-k_{12}\left(\mathbf{L}_A-\lambda\mathbf{I}\right)^{-1}\right) & 0 \\ 0 & \mathbf{I}-k_{34}\left(\mathbf{L}_C-\lambda\mathbf{I}\right)^{-1}\left(\mathbf{I}-k_{43}\left(\mathbf{L}_D-\lambda\mathbf{I}\right)^{-1}\right) \end{pmatrix}-\begin{pmatrix} \left(\mathbf{L}_B-\lambda\mathbf{I}\right)^{-1} \\ \left(\mathbf{L}_C-\lambda\mathbf{I}\right)^{-1} \end{pmatrix}\begin{pmatrix} k_{13} & k_{31} \end{pmatrix}\right|
\end{aligned}
\tag{S3}
$$

The third and last application of the matrix determinant lemma yields:

$$
\begin{aligned}
0 &= \left|\mathbf{L}_A-\lambda\mathbf{I}\right|\left|\mathbf{L}_B-\lambda\mathbf{I}\right|\left|\mathbf{L}_C-\lambda\mathbf{I}\right|\left|\mathbf{L}_D-\lambda\mathbf{I}\right|\left|\mathbf{I}-k_{12}\left(\mathbf{L}_A-\lambda\mathbf{I}\right)^{-1}\right|\left|\mathbf{I}-k_{43}\left(\mathbf{L}_D-\lambda\mathbf{I}\right)^{-1}\right| \\
&\times\left|\mathbf{I}-k_{21}\left(\mathbf{L}_B-\lambda\mathbf{I}\right)^{-1}\left(\mathbf{I}-k_{12}\left(\mathbf{L}_A-\lambda\mathbf{I}\right)^{-1}\right)^{-1}\right|\left|\mathbf{I}-k_{34}\left(\mathbf{L}_C-\lambda\mathbf{I}\right)^{-1}\left(\mathbf{I}-k_{43}\left(\mathbf{L}_D-\lambda\mathbf{I}\right)^{-1}\right)^{-1}\right| \\
&\times\left|\mathbf{I}-\begin{pmatrix} k_{13} & k_{31} \end{pmatrix}\begin{pmatrix} \left(\mathbf{I}-k_{21}\left(\mathbf{L}_B-\lambda\mathbf{I}\right)^{-1}\left(\mathbf{I}-k_{12}\left(\mathbf{L}_A-\lambda\mathbf{I}\right)^{-1}\right)^{-1}\right)^{-1} & 0 \\ 0 & \left(\mathbf{I}-k_{34}\left(\mathbf{L}_C-\lambda\mathbf{I}\right)^{-1}\left(\mathbf{I}-k_{43}\left(\mathbf{L}_D-\lambda\mathbf{I}\right)^{-1}\right)^{-1}\right)^{-1} \end{pmatrix}\right. \\
&\left.\times\begin{pmatrix} \left(\mathbf{L}_B-\lambda\mathbf{I}\right)^{-1} \\ \left(\mathbf{L}_C-\lambda\mathbf{I}\right)^{-1} \end{pmatrix}\right| \\
&= \left|\mathbf{L}_A-\lambda\mathbf{I}\right|\left|\mathbf{L}_B-\lambda\mathbf{I}\right|\left|\mathbf{L}_C-\lambda\mathbf{I}\right|\left|\mathbf{L}_D-\lambda\mathbf{I}\right|\left|\mathbf{I}-k_{12}\left(\mathbf{L}_B-\lambda\mathbf{I}\right)^{-1}\right|\left|\mathbf{I}-k_{43}\left(\mathbf{L}_D-\lambda\mathbf{I}\right)^{-1}\right| \\
&\times\left|\mathbf{I}-k_{21}\left(\mathbf{L}_B-\lambda\mathbf{I}\right)^{-1}\left(\mathbf{I}-k_{12}\left(\mathbf{L}_A-\lambda\mathbf{I}\right)^{-1}\right)^{-1}\right|\left|\mathbf{I}-k_{34}\left(\mathbf{L}_C-\lambda\mathbf{I}\right)^{-1}\left(\mathbf{I}-k_{43}\left(\mathbf{L}_D-\lambda\mathbf{I}\right)^{-1}\right)^{-1}\right|
\end{aligned}
$$

$$
\begin{aligned}
&\times\begin{vmatrix}\mathbf{I}-k_{13}\left(\mathbf{I}-k_{21}\left(\mathbf{L}_B-\lambda\mathbf{I}\right)^{-1}\left(\mathbf{I}-k_{12}\left(\mathbf{L}_A-\lambda\mathbf{I}\right)^{-1}\right)^{-1}\right)^{-1}\left(\mathbf{L}_B-\lambda\mathbf{I}\right)^{-1}\\ -k_{31}\left(\mathbf{I}-k_{34}\left(\mathbf{L}_C-\lambda\mathbf{I}\right)^{-1}\left(\mathbf{I}-k_{43}\left(\mathbf{L}_D-\lambda\mathbf{I}\right)^{-1}\right)^{-1}\right)^{-1}\left(\mathbf{L}_C-\lambda\mathbf{I}\right)^{-1}\end{vmatrix}\\
&=\left|\left(\mathbf{L}_A-\lambda\mathbf{I}\right)\left(\mathbf{I}-k_{12}\left(\mathbf{L}_A-\lambda\mathbf{I}\right)^{-1}\right)\right|\left|\left(\mathbf{L}_D-\lambda\mathbf{I}\right)\left(\mathbf{I}-k_{43}\left(\mathbf{L}_D-\lambda\mathbf{I}\right)^{-1}\right)^{-1}\right|\\
&\left|\left(\mathbf{L}_B-\lambda\mathbf{I}\right)-k_{21}\left(\mathbf{I}-k_{12}\left(\mathbf{L}_A-\lambda\mathbf{I}\right)^{-1}\right)^{-1}\right|\left|\left(\mathbf{L}_C-\lambda\mathbf{I}\right)-k_{34}\left(\mathbf{I}-k_{43}\left(\mathbf{L}_D-\lambda\mathbf{I}\right)^{-1}\right)^{-1}\right|\\
&\times\begin{vmatrix}\mathbf{I}-k_{13}\left(\mathbf{I}-k_{21}\left(\mathbf{L}_B-\lambda\mathbf{I}\right)^{-1}\left(\mathbf{I}-k_{12}\left(\mathbf{L}_A-\lambda\mathbf{I}\right)^{-1}\right)^{-1}\right)^{-1}\left(\mathbf{L}_B-\lambda\mathbf{I}\right)^{-1}\\ -k_{31}\left(\mathbf{I}-k_{34}\left(\mathbf{L}_C-\lambda\mathbf{I}\right)^{-1}\left(\mathbf{I}-k_{43}\left(\mathbf{L}_D-\lambda\mathbf{I}\right)^{-1}\right)^{-1}\right)^{-1}\left(\mathbf{L}_C-\lambda\mathbf{I}\right)^{-1}\end{vmatrix}\\
&=\left|\left(\mathbf{L}_A-\lambda\mathbf{I}-k_{12}\mathbf{I}\right)\left(\left(\mathbf{L}_B-\lambda\mathbf{I}\right)-k_{21}\left(\mathbf{I}-k_{12}\left(\mathbf{L}_A-\lambda\mathbf{I}\right)^{-1}\right)^{-1}\right)\right|\\
&\times\left|\left(\mathbf{L}_D-\lambda\mathbf{I}-k_{43}\mathbf{I}\right)\left(\left(\mathbf{L}_C-\lambda\mathbf{I}\right)-k_{34}\left(\mathbf{I}-k_{43}\left(\mathbf{L}_D-\lambda\mathbf{I}\right)^{-1}\right)^{-1}\right)\right|\\
&\times\begin{vmatrix}\mathbf{I}-k_{13}\left(\mathbf{I}-k_{21}\left(\mathbf{L}_B-\lambda\mathbf{I}\right)^{-1}\left(\mathbf{I}-k_{12}\left(\mathbf{L}_A-\lambda\mathbf{I}\right)^{-1}\right)^{-1}\right)^{-1}\left(\mathbf{L}_B-\lambda\mathbf{I}\right)^{-1}\\ -k_{31}\left(\mathbf{I}-k_{34}\left(\mathbf{L}_C-\lambda\mathbf{I}\right)^{-1}\left(\mathbf{I}-k_{43}\left(\mathbf{L}_D-\lambda\mathbf{I}\right)^{-1}\right)^{-1}\right)^{-1}\left(\mathbf{L}_C-\lambda\mathbf{I}\right)^{-1}\end{vmatrix}\\
&=\begin{vmatrix}\left\{\left(\mathbf{L}_A-\lambda\mathbf{I}-k_{12}\mathbf{I}\right)\left(\mathbf{L}_B-\lambda\mathbf{I}\right)-k_{21}\left(\mathbf{L}_A-\lambda\mathbf{I}\right)\right\}\left\{\left(\mathbf{L}_D-\lambda\mathbf{I}-k_{43}\mathbf{I}\right)\left(\mathbf{L}_C-\lambda\mathbf{I}\right)-k_{34}\left(\mathbf{L}_D-\lambda\mathbf{I}\right)\right\}\\ -k_{13}\left(\mathbf{L}_A-\lambda\mathbf{I}-k_{12}\mathbf{I}\right)\left(\left(\mathbf{L}_D-\lambda\mathbf{I}-k_{43}\mathbf{I}\right)\left(\mathbf{L}_C-\lambda\mathbf{I}\right)-k_{34}\left(\mathbf{L}_D-\lambda\mathbf{I}\right)\right)\\ -k_{31}\left(\mathbf{L}_D-\lambda\mathbf{I}-k_{43}\mathbf{I}\right)\left(\left(\mathbf{L}_A-\lambda\mathbf{I}-k_{12}\mathbf{I}\right)\left(\mathbf{L}_B-\lambda\mathbf{I}\right)-k_{21}\left(\mathbf{L}_A-\lambda\mathbf{I}\right)\right)\end{vmatrix}\\
&=\left|\left(\mathbf{L}'_A-\lambda\mathbf{I}\right)\left(\mathbf{L}'_B-\lambda\mathbf{I}\right)\left(\mathbf{L}'_C-\lambda\mathbf{I}\right)\left(\mathbf{L}'_D-\lambda\mathbf{I}\right)\right|+k_{12}k_{21}k_{34}k_{43}\mathbf{I}-k_{34}k_{43}\left|\left(\mathbf{L}'_A-\lambda\mathbf{I}\right)\left(\mathbf{L}'_B-\lambda\mathbf{I}\right)\right|\\
&-k_{13}k_{31}\left|\left(\mathbf{L}'_A-\lambda\mathbf{I}\right)\left(\mathbf{L}'_D-\lambda\mathbf{I}\right)\right|-k_{12}k_{21}\left|\left(\mathbf{L}'_C-\lambda\mathbf{I}\right)\left(\mathbf{L}'_D-\lambda\mathbf{I}\right)\right|
\end{aligned}
\tag{S4}
$$

Expanding the above expression and collecting powers of λ yields:

$$
\begin{aligned}
0=\;&\mathbf{L}'_A\mathbf{L}'_B\mathbf{L}'_C\mathbf{L}'_D-k_{34}k_{43}\mathbf{L}'_A\mathbf{L}'_B-k_{13}k_{31}\mathbf{L}'_C\mathbf{L}'_D+k_{12}k_{21}k_{34}k_{43}\\
&-\lambda\begin{Bmatrix}\mathbf{L}'_A\mathbf{L}'_B\mathbf{L}'_C+\mathbf{L}'_A\mathbf{L}'_B\mathbf{L}'_D+\mathbf{L}'_A\mathbf{L}'_C\mathbf{L}'_D+\mathbf{L}'_B\mathbf{L}'_C\mathbf{L}'_D\\ -\left(k_{13}k_{31}+k_{34}k_{43}\right)\mathbf{L}'_A-k_{34}k_{43}\mathbf{L}'_B-k_{13}k_{31}\mathbf{L}'_C-\left(k_{12}k_{21}+k_{13}k_{31}\right)\mathbf{L}'_D\end{Bmatrix}\\
&+\lambda^2\left\{\sum_{\substack{i,j\\ j>i}}\mathbf{L}'_i\mathbf{L}'_j-k_{12}k_{21}-k_{13}k_{31}-k_{34}k_{43}\right\}+\lambda^3\left\{\mathbf{L}'_A+\mathbf{L}'_B+\mathbf{L}'_C+\mathbf{L}'_D\right\}+\lambda^4
\end{aligned}
\tag{S5}
$$

Keeping only the three lowest order terms in λ yields Eq. (42).

II. Woodbury approximation for the triangular three-site scheme

In the following, "first" refers to the first order approximation, "second" to the second order approximation. The first order approximation of R_{ex} in a triangular three-site exchange situation can be written as (Eq. 48)

$$R_{ex}^{triang,first} = R_{ex}^{linear,first}\left[\frac{1}{1+\sin^2\theta R_{ex}^{linear,first} Tr\{\mathbf{Z}\}}\right] \tag{S6}$$

The inverse of R_{ex} is:

$$\frac{1}{R_{ex}^{triang,first}} = \frac{1}{R_{ex}^{linear,first}}\left[1+\sin^2\theta R_{ex}^{linear,first} Tr\{\mathbf{Z}\}\right] \tag{S7}$$

The absolute value of differences of reciprocal R_{ex} values can be used to obtain a new approximation for $R_{ex}^{triang,exact}$, which we call $R_{ex}^{triang,new}$:

$$\begin{aligned}&\left|\frac{1}{R_{ex}^{triang,new}}-\frac{1}{R_{ex}^{triang,exact}}\right| < \left|\frac{1}{R_{ex}^{triang,first}}-\frac{1}{R_{ex}^{triang,exact}}\right| \\ &\Leftrightarrow \left|\frac{1}{R_a}\left[1+\sin^2\theta R_b Tr\{\mathbf{Z}\}\right]-\frac{1}{R_{ex}^{triang,exact}}\right| < \left|\frac{1}{R_{ex}^{triang,first}}-\frac{1}{R_{ex}^{triang,exact}}\right|\end{aligned} \tag{S8}$$

in which R_a and R_b must be determined and in which vertical bars denote absolute values. The two cases in which $R_{ex}^{triang,new}$ is smaller or larger than $R_{ex}^{triang,exact}$ must be considered separately. Note that $R_{ex}^{triang,exact} > R_{ex}^{triang,first}$ and $R_{ex}^{linear,exact} > R_{ex}^{linear,first}$.

In the first case, $R_{ex}^{triang,new} < R_{ex}^{triang,exact}$ and $R_{ex}^{triang,first} < R_{ex}^{triang,exact}$:

$$\begin{aligned}&\frac{1}{R_a}\left[1+\sin^2\theta R_b Tr\{\mathbf{Z}\}\right]-\frac{1}{R_{ex}^{triang,exact}} < \frac{1}{R_{ex}^{triang,first}}-\frac{1}{R_{ex}^{triang,exact}} \\ &\Leftrightarrow \frac{1}{R_a}\left[1+\sin^2\theta R_b Tr\{\mathbf{Z}\}\right] < \frac{1}{R_{ex}^{triang,first}}\end{aligned} \tag{S9}$$

Setting R_a to $R_{ex}^{linear,exact}$ and R_b to $R_{ex}^{linear,first}$ yields

$$\frac{1}{R_{ex}^{linear,exact}} < \frac{1}{R_{ex}^{linear,first}} \Leftrightarrow R_{ex}^{linear,exact} > R_{ex}^{linear,first} \tag{S10}$$

which is true as noted above. Setting both R_a and R_b to $R_{ex}^{linear,exact}$ usually violates the condition $R_{ex}^{triang,new} < R_{ex}^{triang,exact}$, as shown empirically.

In the second case, $R_{ex}^{triang,new} > R_{ex}^{triang,exact}$ and $R_{ex}^{triang,first} < R_{ex}^{triang,exact}$:

$$\begin{aligned} &-\frac{1}{R_a}\left[1+\sin^2\theta R_b Tr\left\{\mathbf{Z}\right\}\right]+\frac{1}{R_{ex}^{triang,exact}} < \frac{1}{R_{ex}^{triang,first}}-\frac{1}{R_{ex}^{triang,exact}} \\ &\Leftrightarrow \frac{2}{R_{ex}^{triang,exact}}-\frac{1}{R_{ex}^{triang,first}} < \frac{1}{R_a}\left[1+\sin^2\theta R_b Tr\left\{\mathbf{Z}\right\}\right] \\ &\Leftrightarrow \frac{2}{R_{ex}^{triang,exact}}-\frac{1}{R_{ex}^{triang,first}} < \frac{1}{R_a}+\frac{R_b}{R_a}\left[\frac{1}{R_{ex}^{triang,first}}-\frac{1}{R_{ex}^{linear,first}}\right] \end{aligned} \tag{S11}$$

Again, setting $R_a = R_{ex}^{linear,exact}$ and $R_b = R_{ex}^{linear,first}$ yields:

$$\begin{aligned} &\frac{2}{R_{ex}^{triang,exact}}-\frac{1}{R_{ex}^{triang,first}} < \frac{1}{R_{ex}^{linear,exact}}+\frac{R_{ex}^{linear,first}}{R_{ex}^{linear,exact}R_{ex}^{triang,first}}-\frac{1}{R_{ex}^{linear,exact}} \\ &\Leftrightarrow \frac{2}{R_{ex}^{triang,exact}} < \frac{R_{ex}^{linear,first}}{R_{ex}^{linear,exact}R_{ex}^{triang,first}}+\frac{1}{R_{ex}^{triang,first}} \\ &\Leftrightarrow \frac{R_{ex}^{triang,first}}{R_{ex}^{triang,exact}} < \frac{R_{ex}^{linear,first}}{2R_{ex}^{linear,exact}}+\frac{1}{2} \end{aligned} \tag{S12}$$

which establishes a boundary condition that is frequently, but not always met. In contrast, setting $a = R_{ex}^{linear,exact}$ and $b = R_{ex}^{linear,exact}$ lead to a boundary condition, which is, as empirically shown, usually not met:

$$\begin{aligned}
&\frac{2}{R_{ex}^{triang,exact}} - \frac{1}{R_{ex}^{triang,first}} < \frac{1}{R_{ex}^{linear,exact}} + \frac{1}{R_{ex}^{triang,first}} - \frac{1}{R_{ex}^{linear,first}} \\
&\Leftrightarrow \frac{2}{R_{ex}^{triang,exact}} + \frac{1}{R_{ex}^{linear,first}} < \frac{2}{R_{ex}^{triang,first}} + \frac{1}{R_{ex}^{linear,exact}} \\
&\Leftrightarrow 2\left(\frac{1}{R_{ex}^{triang,exact}} - \frac{1}{R_{ex}^{triang,first}}\right) > \frac{1}{R_{ex}^{linear,exact}} - \frac{1}{R_{ex}^{linear,first}}
\end{aligned} \tag{S13}$$

The new approximation for the triangular three-site scheme performs better than the first-order approximation if the boundary condition Eq. S12 is met.

As a result of the above considerations, the new approximation for R_{ex} is:

$$R_{ex}^{triang,new} = R_{ex}^{linear,exact}\left[\frac{1}{1+\sin^2\theta R_{ex}^{linear,first} Tr\{\mathbf{Z}\}}\right] \tag{S14}$$

and $R_{ex}^{linear,exact}$ can be substituted by $R_{ex}^{linear,second}$, giving the Woodbury approximation:

$$R_{ex}^{triang,Woodbury} = R_{ex}^{linear,second}\left[\frac{1}{1+\sin^2\theta R_{ex}^{linear,first} Tr\{\mathbf{Z}\}}\right] \tag{S15}$$

III. Fitting three-state models

Aspects of using the above expressions for fitting to experimental data are described below for three-state models; extension to more complex topologies are straightforward. The exchange contribution to relaxation is

$$-\lambda = \sin^2\theta R_{ex} = -1/Tr\left\{\left(\mathbf{L}+\mathbf{K}\right)^{-1}\right\} \tag{S16}$$

and for a triangular three-state model,

$$\mathbf{L} = \begin{bmatrix} \mathbf{L}_A & \mathbf{0} & \mathbf{0} \\ \mathbf{0} & \mathbf{L}_B & \mathbf{0} \\ \mathbf{0} & \mathbf{0} & \mathbf{L}_C \end{bmatrix} \tag{S17}$$

in which

$$\begin{aligned} L_A &= \begin{bmatrix} 0 & -\delta_A & 0 \\ \delta_A & 0 & -\omega_1 \\ 0 & \omega_1 & 0 \end{bmatrix} \\ &= \begin{bmatrix} 0 & -\Delta\Omega + p_B\Omega_{BA} + (1-p_A-p_B)\,\Omega_{CA} & 0 \\ \Delta\Omega - p_B\Omega_{BA} - (1-p_A-p_B)\,\Omega_{CA} & 0 & -\omega_1 \\ 0 & \omega_1 & 0 \end{bmatrix} \\ L_B &= \begin{bmatrix} 0 & -\delta_B & 0 \\ \delta_B & 0 & -\omega_1 \\ 0 & \omega_1 & 0 \end{bmatrix} \\ &= \begin{bmatrix} 0 & -\Delta\Omega - (1-p_B)\,\Omega_{BA} + (1-p_A-p_B)\,\Omega_{CA} & 0 \\ \Delta\Omega + (1-p_B)\,\Omega_{BA} - (1-p_A-p_B)\,\Omega_{CA} & 0 & -\omega_1 \\ 0 & \omega_1 & 0 \end{bmatrix} \\ L_C &= \begin{bmatrix} 0 & -\delta_C & 0 \\ \delta_C & 0 & -\omega_1 \\ 0 & \omega_1 & 0 \end{bmatrix} \\ &= \begin{bmatrix} 0 & -\Delta\Omega + p_B\Omega_{BA} - (p_A+p_B)\,\Omega_{CA} & 0 \\ \Delta\Omega - p_B\Omega_{BA} + (p_A+p_B)\,\Omega_{CA} & 0 & -\omega_1 \\ 0 & \omega_1 & 0 \end{bmatrix} \end{aligned} \tag{S18}$$

$$\mathbf{K} = \begin{bmatrix} -k_{12} - k_{13} & k_{21} & k_{31} \\ k_{12} & -k_{21} - k_{23} & k_{32} \\ k_{13} & k_{23} & -k_{31} - k_{32} \end{bmatrix} \otimes \mathbf{I}$$

$$= \begin{bmatrix} -\frac{p_B k_{AB}}{p_A + p_B} - \frac{(1 - p_A - p_B) k_{AC}}{1 - p_B} & \frac{p_A k_{AB}}{p_A + p_B} & \frac{p_A k_{AC}}{1 - p_B} \\ \frac{p_B k_{AB}}{p_A + p_B} & -\frac{p_A k_{AB}}{p_A + p_B} - \frac{(1 - p_A - p_B) k_{BC}}{1 - p_A} & \frac{p_B k_{BC}}{1 - p_A} \\ \frac{(1 - p_A - p_B) k_{AC}}{1 - p_B} & \frac{(1 - p_A - p_B) k_{BC}}{1 - p_A} & -\frac{p_A k_{AC}}{1 - p_B} - \frac{p_B k_{BC}}{1 - p_A} \end{bmatrix} \otimes \mathbf{I} \qquad \text{(S19)}$$

$\Omega_{mA} = \Omega_m - \Omega_A$, $k_{AB} = k_{12} + k_{21}$, $k_{AC} = k_{13} + k_{31}$, and $k_{BC} = k_{23} + k_{32}$.

In the above equations, the known quantities are $\Delta\Omega$ and ω_1; the parameters to be optimized are p_A, p_B, Ω_{AB}, Ω_{AC}, k_{AB}, k_{AC}, and k_{BC}. Use of these variables incorporates the constraints that $p_A + p_B + p_C = 1$ and that the change in free-energy around the reaction cycle must be zero (which constrains k_{23}/k_{32} given the other rate constants). The exchange matrix for the linear three-site model in which A is the middle state (A exchanges with B and C) is obtained by setting $k_{BC} = 0$. The exchange matrix for the linear three-site model in which A is the end state (A exchanges with B and B exchanges with C) is obtained by setting $k_{AC} = 0$. In practice, independent estimates of some of these parameters, such as limiting chemical shifts, may be necessary to reduce the complexity of data fitting. The derivative of $\sin^2\theta\, R_{ex}$ with respect to a parameter x is:

$$\frac{d\left(\sin^2\theta R_{ex}\right)}{dx} = \frac{Tr\left\{\left(\mathbf{L}+\mathbf{K}\right)^{-2} \frac{d\left(\mathbf{L}+\mathbf{K}\right)}{dx}\right\}}{Tr^2\left\{\left(\mathbf{L}+\mathbf{K}\right)^{-1}\right\}} \qquad \text{(S20)}$$

which is needed for gradient-based optimization methods. The derivative on the right-hand-side of Eq. S20 is obtained analytically from Eqs. S16-S19. For example,

$$\frac{d\left(\mathbf{L}+\mathbf{K}\right)}{d\Omega_{BA}}=\begin{bmatrix}\frac{d\mathbf{L}_A}{d\Omega_{BA}} & \mathbf{0} & \mathbf{0}\\ \mathbf{0} & \frac{d\mathbf{L}_B}{d\Omega_{BA}} & \mathbf{0}\\ \mathbf{0} & \mathbf{0} & \frac{d\mathbf{L}_C}{d\Omega_{BA}}\end{bmatrix} \tag{S21}$$

$$\frac{d\mathbf{L}_A}{d\Omega_{BA}}=\begin{bmatrix}0 & -p_B & 0\\ p_B & 0 & 0\\ 0 & 0 & 0\end{bmatrix}$$

$$\frac{d\mathbf{L}_B}{d\Omega_{BA}}=\begin{bmatrix}0 & \left(1-p_B\right) & 0\\ -\left(1-p_B\right) & 0 & 0\\ 0 & 0 & 0\end{bmatrix} \tag{S22}$$

$$\frac{d\mathbf{L}_C}{d\Omega_{BA}}=\begin{bmatrix}0 & -p_B & 0\\ p_B & 0 & 0\\ 0 & 0 & 0\end{bmatrix}$$

As another example,

$$\frac{d(\mathbf{L}+\mathbf{K})}{dk_{AB}}=\frac{1}{p_A+p_B}\begin{bmatrix}-p_B & p_A & 0\\ p_B & -p_A & 0\\ 0 & 0 & 0\end{bmatrix}\otimes\mathbf{I} \tag{S23}$$

Note that Equations S16 and S20 are not expanded analytically (that is, algebraic expressions for the matrix inverses are not needed); rather, numerical values are calculated for each combination of parameters directly from these equations.

IV. Supplemental Figure Captions

Figure S1. $R_{1\rho}$ magnetization decay for two-site chemical exchange. Calculations were performed by numerical evaluation of the integrated Bloch-McConnell equation for each decay component in Eq. 6, using $a_i = \mathbf{d}\left|\mathbf{u}_i\right\rangle\left\langle\mathbf{u}_i^{-1}\right|\mathbf{M}(0)$. Parameters used for the calculations were p_A = 0.5, $p_B = 0.5$, $\omega_1 = 100$ s^{-1}, $\Omega_B - \Omega_A = 1000$ s^{-1}, $\Delta\Omega = 500$ s^{-1}, $R_1 = 1.5$ s^{-1}, $R_2 = 11$ s^{-1} and $k_{ex} = k_{12} + k_{21} = 1000$ s^{-1}. Magnetization decay for the components associated with the (a) least negative, real eigenvalue and (b) the second real eigenvalue. (c) and (d) Real-valued magnetization decays obtained by addition of pairs of components for complex conjugate eigenvalues.

Figure S2. Offset dependence of the R_{ex} contribution to $R_{1\rho}$ for three-site exchange in the strong field limit. (Solid) Numerical calculation of $R_{ex} = -\lambda/\sin^2\theta$ from the least negative real eigenvalue of the 9×9 evolution matrix, (dashed) calculation from the first-order approximation from Eqs. 11 , and (dotted) calculation from the second-order approximation from Eqs. 29 and 40. To center the graph, parameters were chosen so that $\delta_A = \Delta\Omega$. Parameters used for the calculations were $p_A = 0.85$, $p_B = 0.10$, $p_C = 0.05$, $k_{12}+k_{21} = 1550$ s^{-1}, $k_{13}+k_{31} = 2500$ s^{-1}, $\omega_1 = 1250$ s^{-1}, $\Omega_B - \Omega_A = 750$ s^{-1}, $\Omega_C - \Omega_A = -1500$ s^{-1}.

Figure S3. Offset dependence of the R_{ex} contribution to $R_{1\rho}$ for linear three-site exchange in which the sites exchange in different exchange regimes. (Solid) Numerical calculation of $R_{ex} = -\lambda/\sin^2\theta$ from the least negative real eigenvalue of the 9×9 evolution matrix, (dashed) calculation from the first-order approximation from Eqs. 11, and (dotted) calculation from the second-order approximation from Eqs. 29 and 40. The inset exemplifies a region in which the results of the calculations differ. To center the graph, parameters were chosen so that $\delta_A = \Delta\Omega$. Parameters used for the calculations were (in partial analogy to Fig. 2) $p_A = 0.95$, $p_B = 0.035$, p_C=0.015, $k_{12}+k_{21} = 200$ s^{-1}, $k_{13}+k_{31} = 5000$ s^{-1}, ω_1= 500 s^{-1}, $\Omega_B - \Omega_A = 1500$ s^{-1}, $\Omega_C - \Omega_A = -3500$ s^{-1}.

Figure S4. Second-order approximations of $R_{1\rho}$ linear three-site exchange at different dominant site populations. (Left) Actual $R_{1\rho}$ plots, (Right) absolute difference between exact numerical and approximate results. (Solid) Numerical calculation of the least negative real eigenvalue of the 9×9 evolution matrix, (dashed) calculation from the second-order approximation from Eqs. 29 and 40, using R_{eff} from Eq. 13, (dotted) calculation from the second-order approximation from Eqs. 29 and 40, using R_{eff} from Eq. 12, (dashed-dotted) calculation from the second-order approximation from Eqs. 29 and 40, but replacing $\mathbf{L}'_k$ with $\mathbf{L}'_k + \mathbf{R}$ in Eq. 40 and not using R_{eff}. To center the graph, parameters were chosen so that $\delta_A = \Delta\Omega$. Parameters used for calculation: $p_B = p_C = (1-p_A)/2$, $k_{12}+k_{21} = 100$ s^{-1}, $k_{13}+k_{31} = 100$ s^{-1}, $\omega_1 = 50$ s^{-1}, $\Omega_B - \Omega_A = -300$ s^{-1}, $\Omega_C - \Omega_A = 300$ s^{-1}, $R_1 = 1$ s^{-1}, $R_2 = 6$ s^{-1}. (a) $p_A = 0.33$; (b) $p_A = 0.9$.

Figure S5. R_{ex} contribution to $R_{1\rho}$ in triangular 3-state chemical exchange. To center the graph, parameters were chosen so that $\delta_A = \Delta\Omega$. Parameters used for all calculations were $p_A = 0.85$, $p_B = 0.1$, $p_C = 0.05$, $k_{12}+k_{21} = 50$ s^{-1}, $k_{13}+k_{31} = 2000$ s^{-1}, $\Omega_B - \Omega_A = -1000$ s^{-1}, $\Omega_C - \Omega_A = 2000$ s^{-1}, $\omega_1 = 500$ s^{-1}. Left: Triangular 3-state chemical exchange scheme and approximations of the R_{ex} contribution. (Solid) Numerical calculation of $R_{ex} = -\lambda/\sin^2\theta$ from the least negative real eigenvalue of the 9×9 evolution matrix, (dashed) calculation from the first order approximation (Eq. 11), (dotted) calculation from the Woodbury approximation (Eq. 50), (dashed-dotted) calculation from a less well performing variation of the Woodbury approximation in which all first order terms are replaced by second order terms; additional parameter: $k_{23}+k_{32} = 700$ s^{-1}. Right: Difference in error (approximation – numerical value) between the Woodbury approximation and the first order approximation. Values greater than 0 mean that the first order approximation is more accurate than the Woodbury approximation. The value of $k_{23}+k_{32}$ has been varied. Smaller rate constants for $k_{23}+k_{32}$, relative to the other kinetic rate constants, give a more accurate Woodbury approximation.

Figure S6. Approximations for the pseudo-kite 4-site scheme at different population levels. To center the graph, parameters were chosen so that $\delta_A = \Delta\Omega$. Parameters used for all calculations were $p_B = 10/16 \cdot (1 - p_A)$, $p_C = 5/16 \cdot (1 - p_A)$, $p_D = 1/16 \cdot (1 - p_A)$, $k_{21}+k_{12} = 140\ s^{-1}$, $k_{31}+k_{13} = 350\ s^{-1}$, $k_{43}+k_{34} = 700\ s^{-1}$, $k_{41}+k_{14}$ (non-linear fragment) $= 350\ s^{-1}$, $\Omega_B - \Omega_A = -850\ s^{-1}$, $\Omega_C - \Omega_A = 2550\ s^{-1}$, $\Omega_D - \Omega_A = -4250\ s^{-1}$, $\omega_1 = 350\ s^{-1}$. Left: 2-dimensional plots showing the performance of the approximations at three different population scenarios. (Solid) Numerical calculation of $R_{ex} = -\lambda/\sin^2\theta$ from the least negative real eigenvalue of the 12×12 evolution matrix of the pseudo-kite four-site scheme, (dashed) calculation from the first order approximation from Eq. 11, (dotted) Woodbury approximation (Eq. 50). Right: 3-dimensional plots showing the performance of the approximations at three different population scenarios ($0.2 \le p_A \le 0.99$). The absolute differences between the numerical result and the first-order approximation (top) and the Woodbury approximation are plotted.

Figure S7. Use of pseudo-sites to calculate the Woodbury approximation for complex schemes. Top: A pseudo-kite 4-site scheme (grey: non-linear component of the scheme) can be collapsed to a linear three-site scheme. In this example, D* is the pseudo-site which has the same chemical shift as site A. The population in D* can be set low and pseudo-exchange rates between A and D can be set to very large numbers. Middle: Equivalence of the linear three-site scheme and the pseudo-kite 4-site scheme. (Solid) Numerical calculation of $R_{ex} = -\lambda/\sin^2\theta$ from the least negative real eigenvalue of the 12×12 evolution matrix of the pseudo-kite four-site scheme, (dashed – overlapping with solid) numerical calculation of the 9×9 evolution matrix of the linear three-site scheme, (dotted) Woodbury approximation (Eq. 50) of the pseudo-kite four-site scheme. To center the graph, parameters were chosen so that $\delta_A = \Delta\Omega$. Parameters used for all calculations were $p_B = 0.1$, $p_C = 0.05$, $k_{12}+k_{21} = 10\ s^{-1}$, $k_{12}+k_{21} = 500\ s^{-1}$, $\omega_1 = 100\ s^{-1}$, $\Omega_B - \Omega_A = -500\ s^{-1}$, $\Omega_C - \Omega_A = 200\ s^{-1}$. Additional parameters for three-site scheme: $p_A = 0.85$. Additional parameters for four-site scheme: $p_A = 0.84999$, $p_D = 0.00001$, $k_{14}+k_{41} = 10000\ s^{-1}$, $k_{34}+k_{43} = 10000\ s^{-1}$, $\Omega_D - \Omega_A =$

0 s^{-1}. Bottom: A pseudo-kite 5-site system can be used to obtain the Woodbury approximation for a star four-site system (grey: non-linear component of the scheme).

Figure S1

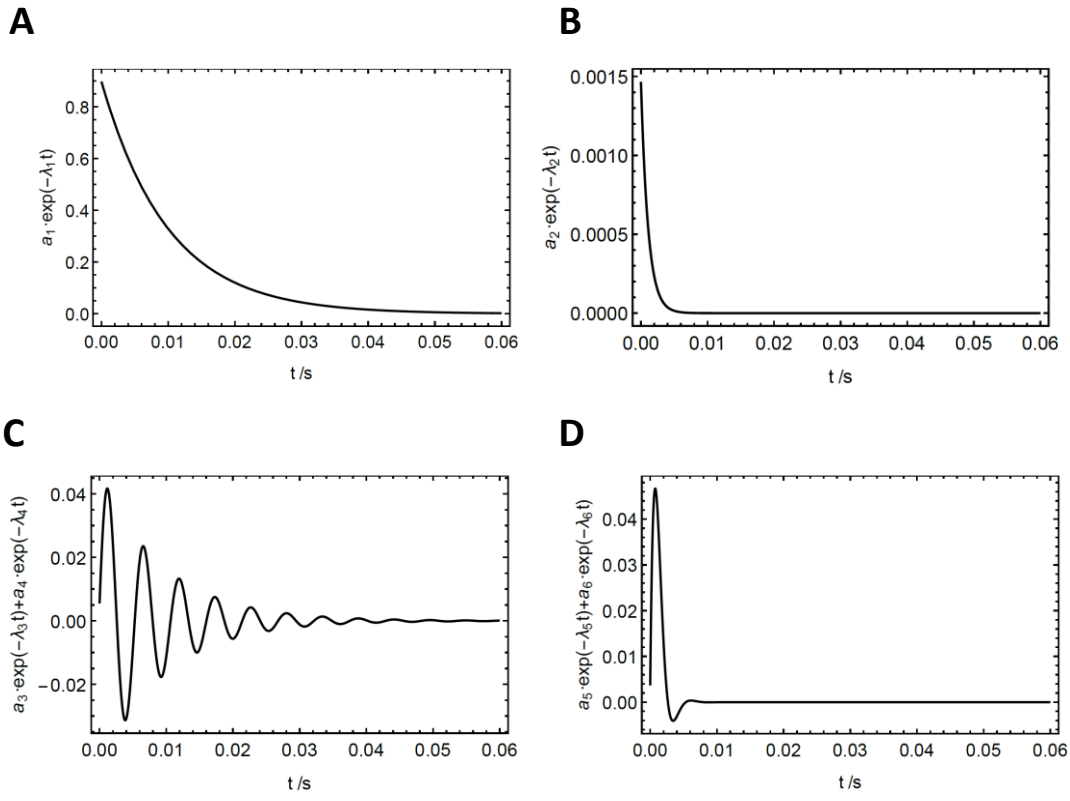
A
B
C
D
$a_1 \cdot \exp(-\lambda_1 t)$
$a_2 \cdot \exp(-\lambda_2 t)$
$a_3 \cdot \exp(-\lambda_3 t) + a_4 \cdot \exp(-\lambda_4 t)$
$a_5 \cdot \exp(-\lambda_5 t) + a_6 \cdot \exp(-\lambda_6 t)$
t /s

Figure S2

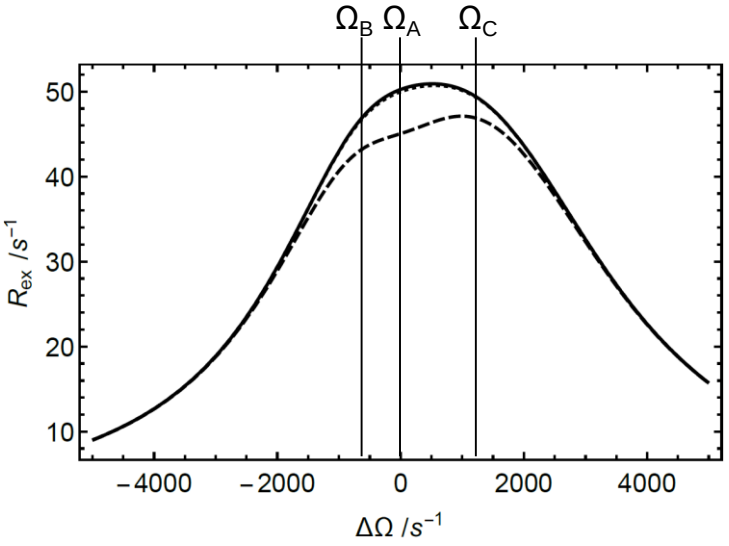
Ω_B Ω_A Ω_C
50
40
30
20
10
R_{ex} /s^{-1}
−4000
−2000
0
2000
4000
$\Delta\Omega$ /s^{-1}

Figure S3

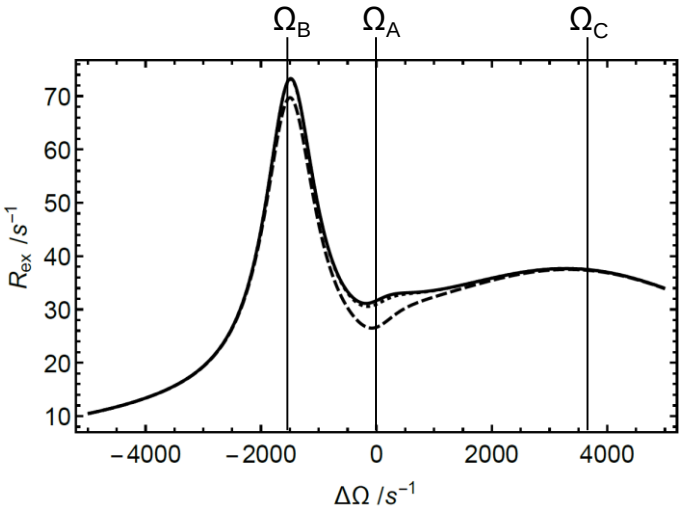
Ω_B
Ω_A
Ω_C
70
60
50
40
30
20
10
R_{ex} /s^{-1}
−4000
−2000
0
2000
4000
$\Delta\Omega$ /s^{-1}

Figure S4

A

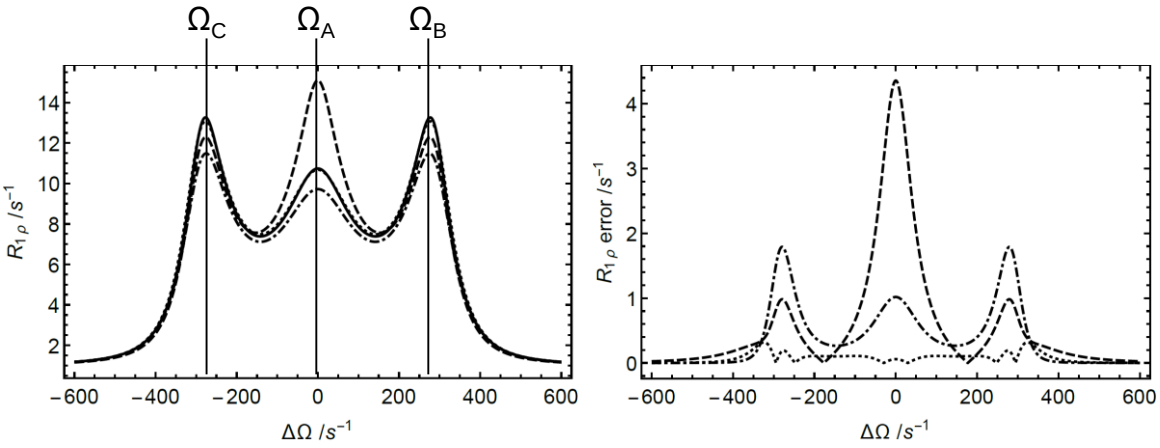
ΩC
ΩA
ΩB
R1ρ /s−1
ΔΩ /s−1
R1ρ error /s−1
ΔΩ /s−1

B

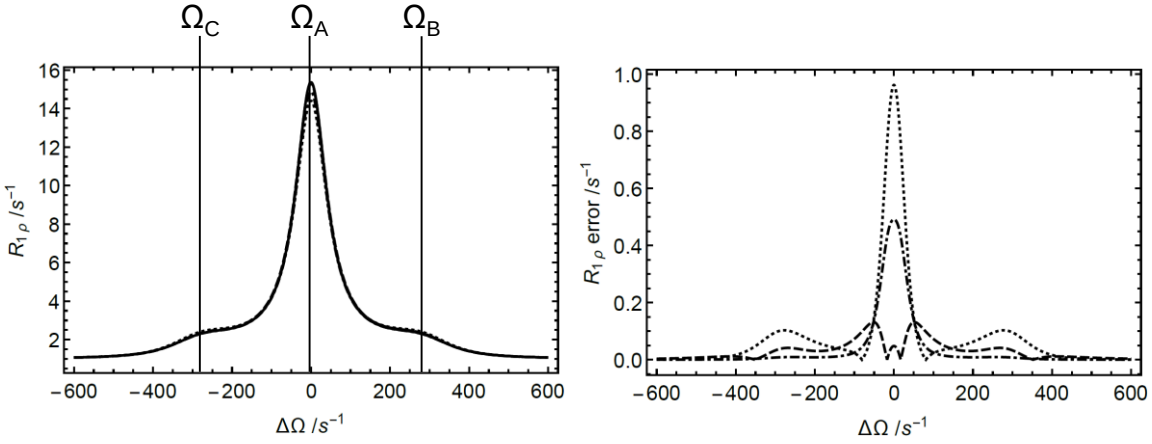
ΩC
ΩA
ΩB
R1ρ /s−1
ΔΩ /s−1
R1ρ error /s−1
ΔΩ /s−1

Figure S5

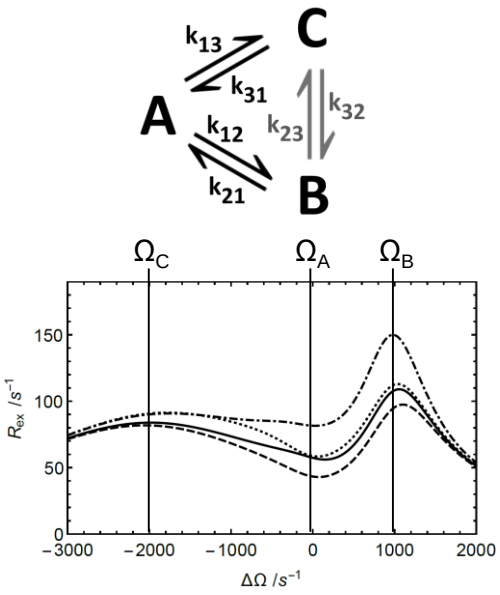
k13
k31
C
A
k12
k23
k32
k21
B
ΩC
ΩA
ΩB
150
100
50
0
Rex /s−1
−3000
−2000
−1000
0
1000
2000
ΔΩ /s−1

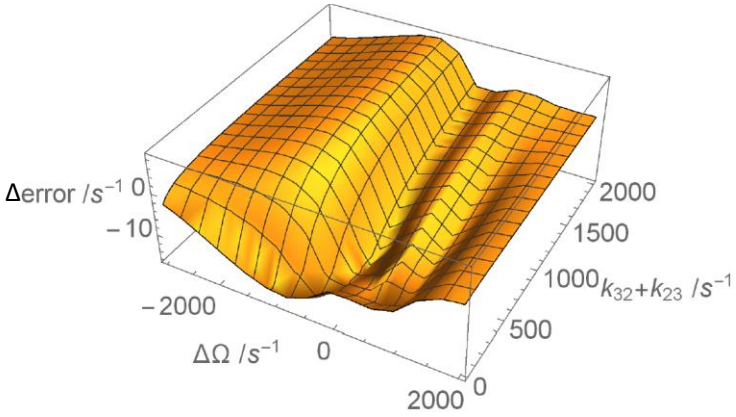
Δerror /s−1
0
−10
−2000
ΔΩ /s−1
0
2000
0
500
1000
1500
2000
k32+k23 /s−1

Figure S6

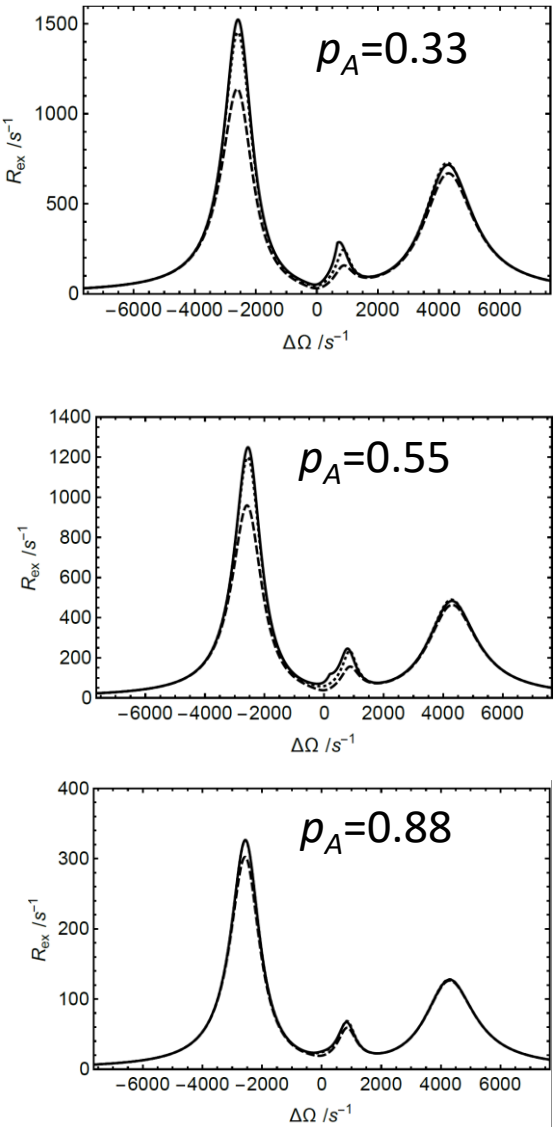
p_A=0.33
R_{ex} /s^{-1}
ΔΩ /s^{-1}
p_A=0.55
R_{ex} /s^{-1}
ΔΩ /s^{-1}
p_A=0.88
R_{ex} /s^{-1}
ΔΩ /s^{-1}

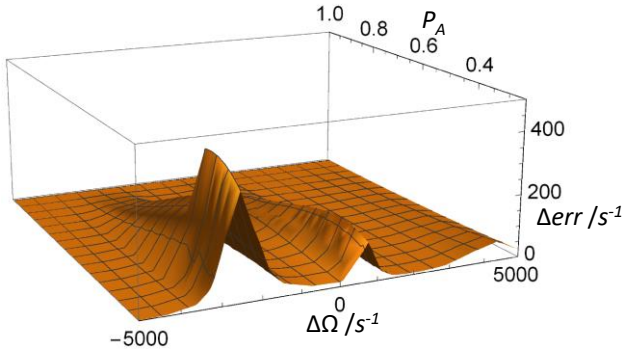
P_A
Δerr /s^{-1}
ΔΩ /s^{-1}

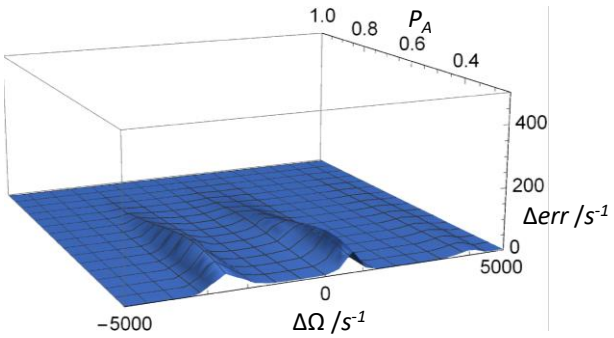
P_A
Δerr /s^{-1}
ΔΩ /s^{-1}

Figure S7

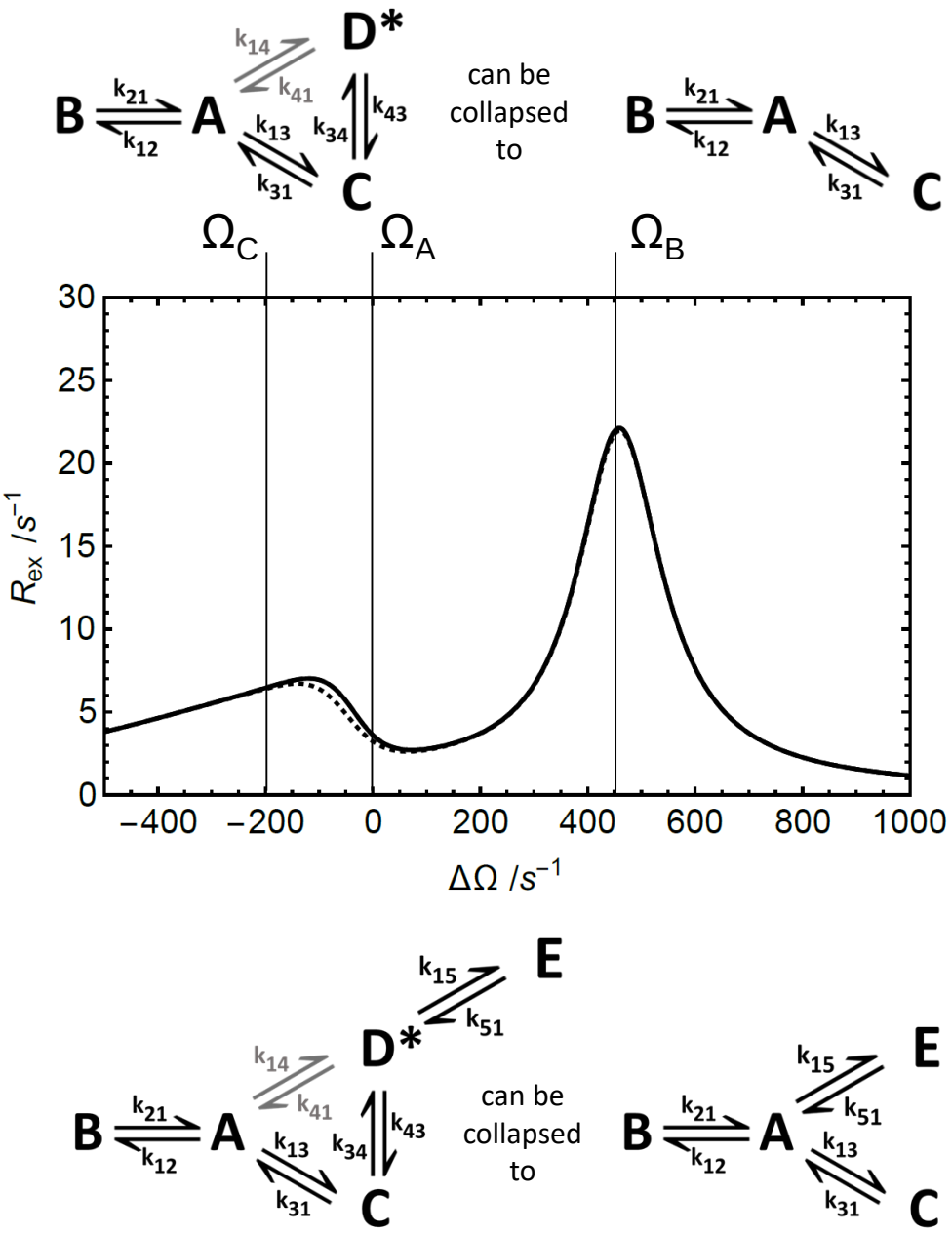
D*
B
A
C
k14
k41
k21
k12
k13
k31
k34
k43
can be collapsed to
ΩC
ΩA
ΩB
30
25
20
15
10
5
0
Rex /s−1
−400
−200
0
200
400
600
800
1000
ΔΩ /s−1
E
k15
k51